An interaction between Sla1p and Sla2p plays a role in regulating actin dynamics and endocytosis in budding yeast

Campbell W. Gourlay, Hilary Dewar, Derek T. Warren, Rosaria Costa, Nilima Satish and Kathryn R. Ayscough*

Institute of Biomedical and Life Sciences, Division of Biochemistry and Molecular Biology, Davidson Building, University of Glasgow, Glasgow, G12 8QQ, Scotland, UK

*Author for correspondence (e-mail: k.ayscough@bio.gla.ac.uk)

Accepted 4 March 2003
Journal of Cell Science 116, 2551-2564 © 2003 The Company of Biologists Ltd
doi:10.1242/jcs.00454

Summary

The importance of a dynamic actin cytoskeleton for facilitating endocytosis has been recognised for many years in budding yeast and is increasingly recognised in mammalian cells. However, the mechanism for actin recruitment and the role it plays in endocytosis is unclear. Here we show the importance of two yeast proteins in this process. We demonstrate that Sla1p and Sla2p interact in vitro and in vivo and that this interaction is mediated by the central domain of Sla2p, which includes its coiled-coil region, and by a domain of Sla1p between residues 118 and 361. Overexpression of the interacting fragment of Sla1p causes reduced fluid-phase endocytosis and, interestingly, defects in subsequent trafficking to vacuoles. We show that Sla2p is required for the polarised localisation of Sla1p in cells but not for its cortical localisation or for its overlapping localisation with actin. Generation of an Δ*sla1*Δ*sla2* double mutant demonstrates that Sla2p is likely to act upstream of Sla1p in endocytosis, whereas sensitivity to latrunculin-A suggests that the proteins have opposite effects on actin dynamics. We propose that Sla2p recruits Sla1p to endocytic sites. Sla1p and its associated protein Pan1p then regulate actin assembly through interactions with Arp2/3 and Arp2/3-activating proteins Abp1p and Las17/Bee1p.

Key words: Sla1p, Sla2p, Actin, Yeast, Endocytosis

Introduction

In yeast, the actin cytoskeleton comprises two types of structure that are visible by fluorescence light microscopy. Actin patches are punctate structures, containing F-actin, that localise to the cell cortex, whereas actin cables are elongated structures that are found throughout the cytoplasm (Adams and Pringle, 1984). A combination of mutational approaches and the effects of actin-disrupting drugs has revealed the importance of the yeast actin cytoskeleton for polarised cell growth, organelle inheritance and endocytosis (Kübler and Riezman, 1993; Novick and Botstein, 1985; Ayscough et al., 1997; Simon et al., 1997). Regulation of cortical actin patch assembly and rearrangement of the actin patches in response to internal and external signals is mediated through interactions of actin with actin-binding proteins, many of which have functional homologues in higher eukaryotic cells (reviewed in Ayscough, 1998). The first actin-binding protein identified and characterised in yeast was Abp1p (Drubin et al., 1988). More recently, a mammalian homologue of Abp1p was identified (mAbp1p). This protein is a signal-responsive F-actin-binding protein that also binds to the endocytic protein dynamin (Kessels et al., 2001). Deletion of *ABP1* in yeast does not have a marked phenotype, which suggests that other proteins may perform overlapping roles with Abp1p. A screen was performed to identify such proteins. Two of the proteins identified were named Sla1p and Sla2p [for synthetically lethal with Abp1p (Holtzman et al., 1993)].

Characterisation of Sla1p has revealed that it is a multivalent adaptor protein required for cortical actin patch structure and organisation in budding yeast (Ayscough et al., 1999). Sla1p has three Src homology-3 (SH3) domains in its N-terminal third and a C-terminal domain composed of multiple repeats rich in proline, glutamine, glycine and threonine (Fig. 1A). These repeats also contain motifs for phosphorylation by the actin-regulating kinase Prk1p (Zeng et al., 2001). We have recently demonstrated that Sla1p can act as an adaptor protein linking the Arp2/3-activating proteins Las17p/Bee1p (the yeast WASP homologue) and Abp1p to the endocytic machinery (Warren et al., 2002).

Sla2p is the yeast homologue of mammalian HIP1 (Huntingtin interacting protein-1), a protein that localises to clathrin-coated pits (Engqvist-Goldstein et al., 1999; Engqvist-Goldstein et al., 2001) (Fig. 1A). Sla2p has an ENTH domain, which, in other proteins, has been shown to interact with membrane inositol phospholipids (De Camilli et al., 2002), and its C-terminal 200 amino acids have homology to talin, another mammalian protein that binds to actin and is found at focal contact sites (Hemmings et al., 1996; Priddle et al., 1998). In vitro, this C-terminal domain of Sla2p is able to bind to actin, and in vivo expression of the C-terminal domain of Sla2p alone localises it to actin structures (McCann and Craig, 1997; Yang et al., 1999). However, the behaviour of other Sla2p mutant proteins in cells suggests, firstly, that Sla2p has a cortical localisation domain in its N-terminus. This is

Table 1. Yeast strains used in this study

Strain	Genotype	Origin/reference
pJ69-2A	MAT**a** *trp1-901, leu2-3,112, ura3-52, his3Δ200*	James et al., 1996
KAY500	pJ69-2A + pKA237	This study
KAY302	MATα *trp1-1, leu 2-3,112, lys2-801, his3-Δ200, ura 3-52*	DDY 852*
KAY303	KAY302 + integrated SLA1-9xmyc::TRP1	This study
KAY367	MATα *trp1-1, his3-Δ200, leu2-3,112, ura 3-52 Δsla1::LEU2, sla1Δ118-511*-9xmyc::*TRP1*	This study
KAY351	MAT**a** *his3-200, leu2-3,112, ura 3-52, sla1Δ::LEU2, sla1(Δ118 - 511)::HIS3*	This study
KAY97	MAT**a**, *sla1-Δ1::URA3, ura 3-52, his3Δ200*	DDY332*
KAY136	MATα *sla2Δ1::URA3, ade2, leu 2-3,112, ura 3-52*	DDY544*
KAY128	MATα *Δsla1::URA3, Δsla2::HIS3, his3-Δ200, leu2-3,112, ura 3-52*	This study
KAY415	MAT**a**, *leu 2, trp 1, ura 3-52, prb 1-1122, pep 4-3, prp 1-451*	DDY1810*
KAY419	KAY 415 + pJC230 (pEG KT + *SLA1*)	This study
KAY 445	*SLA2-6HIS::URA3, ade1-1, his3-Δ200, ura 3-52*	DDY1550*
KAY137	MAT**a**, *his3-Δ200, leu2-3,112, ura 3-52, sla2-Δ1::URA3*	DDY 545*
KAY658	MAT**a**, *leu 2-3,112, lys2-801, his3-Δ200, ura 3-52, SLA1*-9xmyc::*TRP1, sla2-Δ1::URA3*	This study
KAY439	KAY415 + pEG(KT+) expressing GST alone	This study
KAY508	KAY415 + pKA240	This study
KAY657	KAY415 + pKA300	

*D. Drubin (UC Berkeley, CA).

potentially due to the ENTH domain acting to localise the protein to regions of clathrin coats. Secondly, a region upstream of the talin homology region may mask its ability to bind to actin (McCann and Craig, 1997; Wesp et al., 1997; Yang et al., 1999). Thus Sla2p may only bind to actin via its talin-like domain when it is modified (e.g. phosphorylated) or when associated with other proteins that allow appropriate unmasking of the site.

Here we show that Sla1p and Sla2p associate both in vivo using a two-hybrid approach and in vitro using purified proteins. We also define the interacting domain as a stretch of 243 amino acids in Sla1p and of 458 amino acids in the coiled-coil region of Sla2p. The role of this interaction is investigated further using genetic and cell biological approaches. In addition, deletion of either or both genes is detrimental to the ability of cells to undergo endocytosis. Furthermore, in cells lacking both Sla1p and Sla2p, the cortical actin cytoskeleton is unable to polarise, and the majority of actin is localised to the distal end of the cell. On the basis of the experimental data shown here and of results from other published reports we propose a model in which Sla1p acts as a link between Sla2p, clathrin and other endocytic machinery and the cortical actin cytoskeleton. Within this complex Sla1p destabilises and facilitates depolymerisation of F-actin. Sla2p and other proteins may then promote formation of new F-actin structures, which are important for driving endocytosis.

Materials and Methods

Materials

Unless stated otherwise, chemicals were obtained from BDH/Merck or Sigma. Media was from Melford Laboratories (yeast extract, peptone, agar) or Sigma (minimal synthetic medium and amino acids). Latrunculin-A was a gift from Phil Crews (UC Santa Cruz, CA).

Yeast strains and growth conditions

Yeast strains and plasmids used in this study are listed in Table 1 and Table 2, respectively. Unless stated otherwise, cells were grown in a rotary shaker at 30°C in liquid YPD medium (1% yeast extract, 2% Bacto-peptone, 2% glucose supplemented with 40 μg/ml adenine), except for KAY419, KAY439, KAY508 and KAY657 cells, which were grown under selection in synthetic media lacking uracil. Halo assays were performed as previously described (Ayscough et al., 1997). The mutant Sla1Δ118-511 was myc-tagged using oligonucleotides and methods previously described (Warren et al., 2002).

Table 2. Plasmids used in this study

Plasmid	Description	Origin/reference
pJC230	For overexpression of GST-Sla1p (pEG-KT + *SLA1*)	D. Drubin (UC Berkeley, CA)
pGBDU-C1	Yeast 2 hybrid binding domain plasmid	James et al., 1996
pGAD-C1	Yeast 2 hybrid activation domain plasmid	James et al., 1996
pKA51	pRS313 + *SLA1*	Ayscough et al., 1999
pKA116	pRS313 + *SLA1ΔSH3#3*	Ayscough et al., 1999
pKA161	pGEX1+Sla1(118-511ΔSH3#3)	This study
pKA237	pGBDU-C1 + *SLA1*(118-511)	This study
pKA238	pGBDU-C1 + *SLA1*(118-511) with sequence corresponding to SH3#3 excised	This study
pKA283	pGBDU-C1 + *SLA1*(1-361)	This study
pKA244	pGAD + SLA2 (310-768)	This study
pDD375	pACTII + *SLA2*(502-767)	Yang et al., 1999
pDD376	pACTII + *SLA2*(502-767)	Yang et al., 1999
pDD379	pACTII + *SLA2*(502-767)	Yang et al., 1999
pDD381	pACTII + *SLA2*(502-767)	Yang et al., 1999
pRD56	pRS316+GAL1-GST	
pKA240	GST+ Sla1(118-511ΔSH3#3)	This study
pKA300	pKA240 mutated at *Sla1* residues 198(P to N) and 199 (A to S).	This study

Protein purification and interactions

GST alone and GST-Sla1(118-511ΔSH3#3) were expressed from DH5α bacteria by following pGEX vector protocols (Amersham Pharmacia). GST-Sla1 was expressed and purified from 4 l of KAY419 cells as previously described (Warren et al., 2002). SixHis-tagged Sla2p was purified on a Ni-NTA resin column from KAY445 cells as described previously (Yang et al., 1999).

Pulldown assays were carried out with purified GST-Sla1p bound to glutathione Sepharose beads as described previously (Warren et al., 2002). Whole cell lysates were spun at 2000 ***g*** for 4 minutes to remove unbroken cells, and the supernatant spun at 300,000 ***g*** for 20 minutes at 4°C. The final supernatant was removed and 100 μl incubated with either 20 μl of GST-Sla1p coated glutathione beads or with 20 μl of glutathione sepharose for 3 hours at 4°C with rotation. The beads were spun down at 500 ***g*** for 4 minutes and washed three times in 10 bed volumes of binding buffer. Bound proteins were eluted in sample buffer and separated on a 10% SDS polyacrylamide gel before transfer to PVDF for analysis.

Purified 6×His-tagged Sla2p was eluted from Ni-NTA beads in binding buffer (50 mM K-HEPES pH 7.5, 100 mM KCl, 1 mM EDTA, 1 mM EGTA + protease inhibitors as above) + 0.01% Triton X-100. Proteins were eluted from the beads in sample buffer and separated on a 10% SDS polyacrylamide gel before being transferred to PVDF for analysis. Western blotting of purified 6×His-Sla2p revealed that no Sla1p was co-purified (data not shown).

For investigating binding of GST-Sla1(118-511ΔSH3#3) to His-tagged Sla2p, the Sla2p beads were firstly washed in high stringency buffer (2 M NaCl, 2% Triton-X100, 20 mM imidazole, 50 mM NaH_2PO_4 pH8). 25 μl of Sla2p on beads were incubated with GST or GST-Sla1 fragment (final concentration 0.1 mg/ml) in binding buffer (50 mM NaH_2PO_4 pH8, 20 mM imidazole, 0.3 M NaCl) for 3 hours at 4°C. The beads were washed three times in binding buffer and bound proteins were eluted in sample buffer.

Yeast whole cell lysates were prepared as previously described (Warren et al., 2002) and samples were run on 10% SDS polyacrylamide gels. For immunoblots, affinity-purified rabbit anti-yeast Sla2 antibodies (a gift from D. Drubin, UC Berkeley) were diluted 1:500. GST and GST-Sla1p were detected using affinity-purified polyclonal rabbit antiserum against the GST epitope at a 1:1000 dilution. Anti mouse and rabbit HRP-conjugated secondary antibodies (Sigma) were used at 1:5000 and detected using ECL chemiluminescence.

Yeast two-hybrid screen

The yeast two-hybrid screen used bait and activation plasmids and a yeast strain pJ69-2A designed and constructed by Philip James (James et al., 1996). The region of Sla1p to be tested in the two-hybrid assay was subcloned from a plasmid carrying the entire *SLA1* gene [pKA51 (Ayscough et al., 1999)]. *Eco R1* digestion was used to cut out the fragment corresponding to amino acids 118 -511 from the gene, and this fragment was then cloned into the pGBDU-C1 bait vector. The bait plasmid was checked for self-activation before the library screen was carried out. For checking the requirement of the third SH3 domain, *EcoR1* was used to digest plasmid pKA116, which had been constructed previously (Ayscough et al., 1999). This released the fragment as above but without the SH3 domain.

For the screen, 2 μg of bait plasmid (pKA237) was transformed into the two-hybrid yeast strain pJ69-2A to give a strain KAY500. 2×10^9 KAY500 cells, grown in liquid media lacking uracil, were transformed with 20 μg library DNA from each reading frame (library was a gift from Francis Barr, Munich, Germany). In total, the 202 colonies that grew within 7 days were picked from plates lacking histidine, uracil and leucine. Following re-streaking and selection for the inability to grow on media lacking adenine and containing 5-fluororotic-acid (5-FOA), a total of 57 yeast strains remained and plasmids were extracted from these. The plasmids were then re-transformed into pJ69-2A with the bait plasmid to ensure that activation of reporter genes still occurred. Twenty-six of the 57 yeast strains could not grow on activation plates. The remaining 31 plasmids were sequenced to identify the region responsible for the two-hybrid interaction, and the resulting sequence was compared with DNA sequences from *S. cerevisiae* using the BLAST alignment program found at the *Saccharomyces* Genome Database Website (http://genome-www.stanford.edu/Saccharomyces/). The interacting genes identified were YSC84 [17 isolates (Dewar et al., 2002)], SLA2 (7 isolates), SED5 (3 isolates), RAD52 (1 isolate) and non-coding DNA (3 isolates).

Sucrose gradients

Linear sucrose gradients (12 ml of 3-30%) in UBT buffer (50 mM KHEPES, pH 7.5, 100 mM KCl, 3 mM $MgCl_2$, 1 mM EGTA, 0.5% Triton X-100) were prepared in Beckman UltraClear 13 ml centrifuge tubes. Yeast extracts were prepared from 100 ml cultures of KAY303 cells, at an OD600 of 1.0, by liquid nitrogen grinding after harvesting cells at 3000 ***g*** for 4 minutes at 4°C and resuspending the pellet in cold 2×UBT buffer. Ground extracts were thawed at 4°C then subjected to a 3000 ***g*** spin, and the resulting supernatant samples (500 μl) were layered on top of the sucrose gradient spun at 35,000 ***g*** for 18 hours at 4°C. Fractions (250 μl) were removed manually from the bottom of the tube and then assayed by SDS-PAGE. Immunoblotting was used to determine the position of various proteins. For immunoblots, antibodies used were anti-cofilin (1/500), anti-Abp1p (1/1000), anti Sla2p (1/500) – all gifts from D. Drubin (Berkeley, CA); anti-Chc1 (1/100), a gift from Sandra Lemmon (Cleveland, Ohio); anti-actin (1/500), a gift from John Cooper (Washington University, St. Louis); and anti-Sla1 (1/500) (Warren et al., 2002). Quantitation of band intensity was determined using NIH Image 1.6.1 Software.

Fluorescence microscopy

Endocytosis of the fluid phase marker lucifer yellow was performed according to the published method (Dulic et al., 1991), and analysis of the uptake of lipophylic dye FM4-64 was performed as described previously (Vida and Emr, 1995). Rhodamine-phalloidin (Molecular Probes) staining of actin was performed as described elsewhere (Hagan and Ayscough, 2000). Cells were processed for immunofluorescence microscopy as described previously (Ayscough and Drubin, 1998). Antibodies were used to detect Sla2p, Abp1p, Sac6p (a gift from D. Drubin, UC Berkeley, CA), Rvs167p (a gift from H. Friesen, University of Toronto, CA) and the myc epitope (for Sla1p-myc; Santa Cruz Biotech, CA) for immunofluorescence microscopy at 1:100 dilution. Secondary antibodies used were FITC-conjugated goat anti-rabbit (Vector Laboratories) at dilutions of 1:1000. Cells were viewed with an Olympus microscope BX-60 fluorescence microscope with a 100 W mercury lamp and an Olympus 100× Plan-NeoFluar oil-immersion objective. Images were captured using a Roper Scientific Micromax 1401E cooled CCD camera using IP lab software (Scanalytics, Fairfax, VA) on an Apple Macintosh G4 computer.

Electron microscopy

Log phase cells were fixed using freshly prepared 2% potassium permanganate for 45 minutes at room temperature. Following washing the pellets were processed by dehydration through a series of ethanol from 50-100% and then in propylene oxide. Samples were then incubated overnight in a resin (Durcapan):propylene oxide 1:1 mix before embedding in resin and curing. Sections were cut and stained with uranyl acetate and lead citrate before viewing them on a Zeiss 902 transmission electron microscope.

Results

The domain of Sla1p responsible for its role in actin organisation is not required for cortical localisation

In previous studies we demonstrated that deletion of distinct domains of Sla1p affected certain functions of the protein. In particular, the region between amino acids 118 and 511 of the 1244 amino-acid protein was shown to be important for the functions of Sla1p in regulating cortical actin structures (Ayscough et al., 1999). The Sla1p 118-511 region encompasses a region of novel sequence between the second and third SH3 domains (amino acids 118-361), the third SH3 domain (amino acids 362-415) and a further 96 amino acids beyond the third SH3 domain. Deletion of the third SH3 domain did not have a detectable effect on actin structures in cells, indicating that a combination of this and the sequences either side of the SH3 domain are likely to be important for interacting with other cell proteins (Ayscough et al., 1999). To avoid concerns with slight variation in copy number from these studies on plasmid borne mutations, the *sla1Δ118-511* mutant for this study was integrated into the genome and expressed as the sole form of Sla1p in cells. Expression was detected using anti-Sla1p antibodies and was observed to be at similar levels to wild-type protein expression (Fig. 1B).

Our antibodies did not prove useful for indirect fluorescence microscopy so, in order to localise the mutant protein in cells, a myc tag was integrated at the C-terminus of the mutant Sla1Δ118-511p. The myc-tagged protein was also detectable by western blotting and had no observable phenotypes in addition to those of the mutant itself (data not shown). By indirect fluorescence microscopy, Sla1Δ118-511p was observed to localise to small punctate patches at the cell cortex, which indicates that the protein still contains signals required for its localisation to discrete cortical sites in the cell (Fig. 1C). The pattern of staining was not well polarised and does not show the same organisation as actin, which is in large cortical chunks in these cells (Ayscough et al., 1999) (Fig. 5B).

As well as showing that Sla1Δ118-511p is expressed and localises to appropriate regions of the cell, we were also able to show that cells expressing the mutant are able to rescue a phenotype associated with the complete *sla1* deletion. Cells lacking *sla1* cannot grow in the absence of *abp1* expression (deletion of both genes is synthetically lethal). However, a combination of *sla1Δ118-511* and Δ*abp1* is not lethal to cells, which demonstrates, firstly, that the Sla1Δ118-511 protein must be partly functional and, secondly, that the overlapping function with Abp1p lies in another part of the protein. Other work in the laboratory has indicated that this redundancy is attributable to the presence of the C-terminal repeat region of Sla1p (Ayscough et al., 1999). Further analysis of the *sla1Δ118-511* strain showed that it has similar resistance to the effects of the actin-disrupting drug latrunculin-A to cells in which the entire *sla1* gene is deleted. Again, this indicates that the links with the actin cytoskeleton are mediated through this domain of the protein (data not shown).

A two-hybrid screen with the Sla1 118-511 region detects Sla2p as a binding partner

To investigate the role of the Sla1(118-511) region further, a two-hybrid screen was conducted using this sequence as bait.

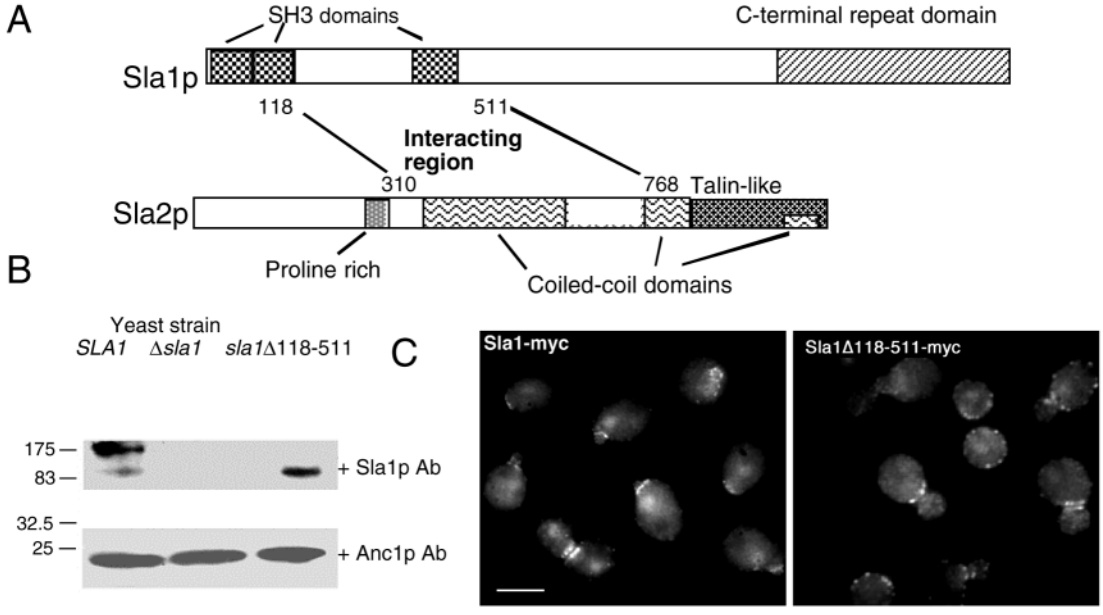

Fig. 1. Sla1Δ118-511p is expressed in cells and localises to the cell cortex. (A) Schematic diagram of Sla1p and Sla2p showing domain structure and regions of Sla1p thought to be important for its role in regulating the actin cytoskeleton. (B) Cells expressing full-length Sla1p, Sla1Δ(118-511)p or cells in which Δ*sla1* was deleted (KAY302, 351 or 97 respectively) were grown overnight and cell extracts made. Proteins were separated by SDS-PAGE and western blotted using antibodies against Sla1p. As shown, proteins of the appropriate size were found in cells expressing Sla1p. No band was observed in the extract from Δ*sla1* cells. As a loading control the same blots were probed with antibodies to a nuclear protein Anc1p. This showed equivalent levels in all lanes. (C) Log phase KAY303 and KAY367 cells expressing Sla1-myc and Sla1Δ(118-511)myc were grown to log phase and processed for immunofluorescence microscopy. Both Sla1p-myc and Sla1Δ(118-511)-myc localise to punctate patches at the cell cortex demonstrating that the parts of Sla1p required for cortical localisation are located elsewhere in the protein. Bar, 5 μM.

Details of the constructs used are given in Materials and Methods. Of 31 positive interactors, seven were subsequently sequenced and shown to encode Sla2p. Within the seven isolates two different start sites at amino acids 204 and 310 were identified, but they all carried the same end site corresponding to amino acid 768 in Sla2p. The minimum interacting sequence was therefore the region between amino acids 310 and 768. This region of Sla2p corresponds to its central domain, which is predicted to be largely coiled-coil in nature (Fig. 1A, Fig. 2A,B) (Wesp et al., 1997; Yang et al., 1999).

To ascertain whether the SH3 domain of Sla1p is important for the interaction with Sla2p, a modified bait plasmid was generated in which the SH3#3 domain is deleted. The two-hybrid transformations were repeated, and an interaction was still found to occur, which indicates that the sequence important for the Sla1p:Sla2p interaction lies outside the third SH3 domain of Sla1p (Fig. 2). Interestingly, this interaction appeared to be stronger than with the construct containing the SH3 domain, which suggests that the domain might normally partly interfere with, or regulate, an Sla1p:Sla2p interaction. In addition, an Sla1p bait plasmid containing the sequence from residue 1 to 361 also interacted with the Sla2p activation plasmid, indicating that the region of Sla1p involved in the interaction with Sla2p lies between residues 118 and 361. Further interactions between Sla1p and Sla2p central domain fragments were also tested (Fig. 2A,B), but none of these yielded a clear positive interaction, which might suggest that the interaction sites require a tertiary structure that cannot be generated by any of the Sla2p fragments.

Sla1p and Sla2p interact in vitro

Although an interaction between Sla1p and Sla2p has been shown through a two-hybrid approach, it is possible that this could occur through an intermediary protein. To investigate this possibility a plasmid expressing GST-Sla1p was transformed into yeast cells and purified from whole cell lysates. Following purification of Sla1p, cell extracts were passed over the protein on a column, and proteins in bound and unbound fractions were separated by SDS-PAGE and transferred to PVDF for analysis. Western blots were probed with antibodies raised against several proteins known to associate with cortical patches. Fig. 3A shows that under these conditions, an interaction was detected between GST-Sla1p and Sla2p.

To establish whether the interaction between Sla1p and Sla2p is likely to be direct and not mediated by an accessory, we purified 6×His-tagged Sla2p and performed a direct in vitro binding assay. The GST-Sla1p beads were blotted prior to Sla2p binding to verify that no Sla2p co-purified in the GST-Sla1p preparation (lower panel Fig. 3B). Fig. 3B clearly demonstrates that Sla1p and Sla2p interact in vitro. The controls presented demonstrate that the pulldown of purified Sla2p by Sla1p-coated beads is not due to the presence of the associated His or GST tags nor is it attributable to the presence of glutathione beads. In both GST pulldown experiments, Coomassie-stained gels showed that proteins other than Sla1p and Sla2p were not present at detectable levels in the purified protein extracts (data not shown).

Finally, an interaction between bacterially expressed GST-Sla1 fragment (118-511) and His-tagged Sla2p was demonstrated (Fig. 3C). Beads carrying Sla2p were washed stringently (in 2 M NaCl) prior to incubating with the GST or GST-Sla1 fragment. This wash removes any interacting proteins that can be detected on gels or by western blotting for specific proteins including Sla1p, Sac6p, actin, cofilin or Abp1p. In fact, a lower stringency wash (0.3 M) is sufficient to disrupt the Sla1p:Sla2p interaction (data not shown). Either GST alone or the GST-Sla1p fragment was incubated with His-tagged Sla2p. As shown in Fig. 3C, the Sla1p fragment, but not GST alone, is able to bind to Sla2p. All other bands on the Coomassie-stained gel were

A

Sla1 Binding Domain Constructs

Sla2 activation domain constructs	pKA237 (118-511)			pGBDU-C1
pKA244 (310-768)	++	+++	+++	-
pDD375 (502-767)	-	-	n.d.	n.d.
pDD376 (575-767)	-	-	n.d.	n.d.
pDD381 (5-358)	-	-	n.d.	n.d.
pDD379 (5-576)	-	-	n.d.	n.d.
pGAD-C1	-	-	-	n.d.

B. – Ura, Leu

C. – His, Ade, Ura, Leu

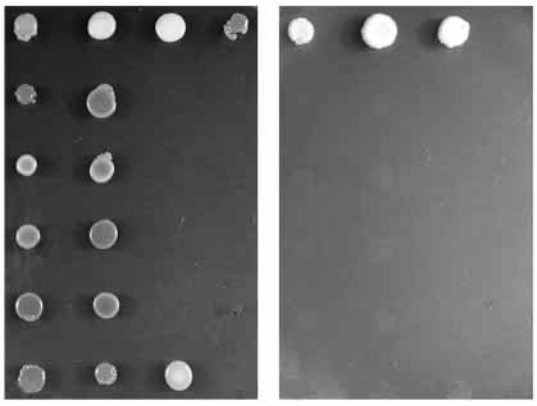

Fig. 2. Sla1p interacts with Sla2p in a two-hybrid screen. A two-hybrid screen was performed as described in Materials and Methods with a bait plasmid carrying the amino acid 118-511 region of Sla1p. The minimum interacting sequence was between residues 310 and 768 of Sla2p. Two-hybrid interactions between a number of different Sla1 and Sla2 constructs were tested, as shown. (A) Summary of domain interactions. The strength of interaction was determined by the extent of growth after 5 days with +++ denoting the greatest growth. Corresponding to positions on this table are strains which in B are growing on synthetic medium lacking uracil and leucine, indicating that both plasmids are present, and in C are growing on synthetic medium lacking histidine, adenine, uracil and leucine, indicating that a positive interaction between Sla1p and Sla2p has taken place.

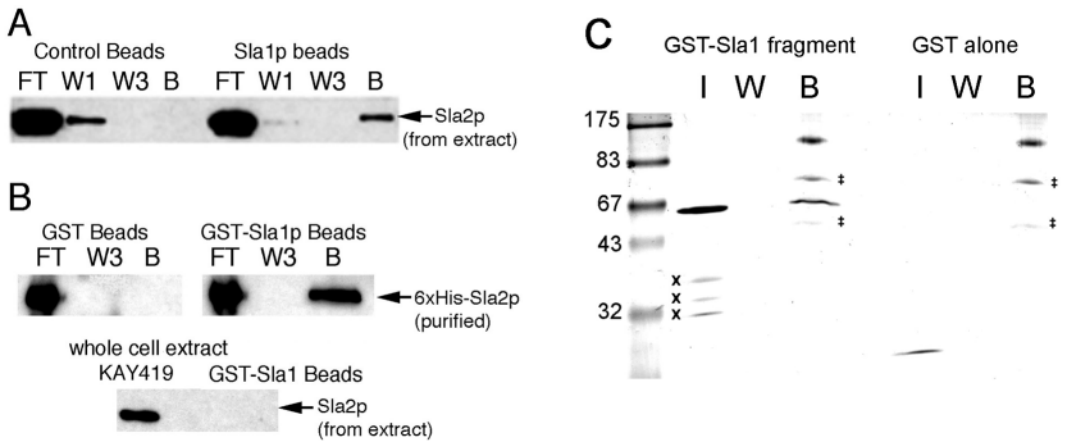

Fig. 3. Sla1p and Sla2p interact in vitro. (A) GST-Sla1p was purified as described in Materials and Methods. Cell extracts were passed over the protein on a column and proteins in bound and unbound fractions were separated by SDS-PAGE and transferred to PVDF for analysis. Western blots were probed with antibodies raised against Sla2p. Sla2p bound only to Sla1p carrying beads and not to control beads alone. FT, flow through; W1,W3, washes 1 and 3; B, bound. (B) To investigate whether the interaction between Sla1p and Sla2p was direct, His-tagged Sla2p was purified from cells as described in Materials and Methods, and its binding to GST control beads or to GST-Sla1p beads was assessed. As shown in the upper panel Sla2p only binds to Sla1p-containing beads. As a control, the extracts from KAY419 cells from which GST-Sla1p was purified were probed to demonstrate the presence of Sla2p in the extract. Then, following GST-Sla1p purification the beads were probed to demonstrate that no Sla2p had co-purified with the Sla1p. Therefore, the Sla1p-Sla2p binding observed was only caused by the presence of the added Sla2p to the GST-Sla1p beads. FT, flow through; W1,W3, washes 1 and 3; B, bound. (C) Bacterially expressed GST or GST-Sla1(118-511ΔSH3#3) was incubated with His-tagged Sla2p as described in Materials and Methods. The beads were washed and the input material (I), wash (W) and bound (B) fractions were run on a gel that was then stained using Coomassie dye. The three bands marked x are all detected by western blotting with GST antibodies indicating that they are all Sla1 degradation products; bands marked ‡ were detectable using Sla2 antibodies.

detectable by western blotting using antibodies against GST (for the GST-Sla1 preparation) or against Sla2p (His-tagged Sla2p preparation), which indicates that the Sla1p:Sla2p interaction is direct.

Fractionation of cell extracts indicates that Sla1p and Sla2p form a complex in vivo

Evidence that Sla1p and Sla2p may form a complex in vivo was produced by carrying out subcellular fractionation of yeast total protein extracts on a 3-30% sucrose gradient (Fig. 4). Fractions taken from the velocity gradient were probed with antibodies raised against Sla2p, Abp1p, actin, cofilin, clathrin heavy chain (Chc1p) and Sla1p. Identical fractionation was also performed on cell extracts from strains lacking *sla1*. A number of significant findings were made. Firstly, there are two peaks that are highly enriched for actin, Abp1p and cofilin (fractions 6-10 and 16-20), indicating these proteins are found in both small and large complexes in the cell. In extracts from wild-type cells, Sla1p and Sla2p are not found in the fraction 6-10 peak but do co-fractionate in the 16-20 peak, which represents larger protein complexes. Clathrin is also found in these same dense fractions. Interestingly, in the absence of Sla1p, the major Sla2p peak is shifted to a less dense fraction, indicating that it may have been part of an Sla1p complex, which is consequently smaller in the absence of this 140 kDa protein. A significant proportion of Sla2p has also moved out of the dense fractions into less dense fractions; 72% of Sla2p is in fractions 14-20 in wild-type cells compared with 43% in Δ*sla1* cells. This indicates that Sla1p is important for maintaining the integrity of the Sla2p complex.

In the wild-type extracts 30% of actin was found in fractions 16-20, this falls to 20% in the absence of *sla1*, also suggesting a role for Sla1p in association of actin with the large complex. These proportional changes in actin and Sla2p fractionation patterns in the presence and absence of Sla1p were reproducible over the three experiments performed. Abp1p is found in two distinct peaks, both in the presence and absence of Sla1p, though in the absence of Sla1p the denser fraction is reduced in size, which indicates that it may have contained Sla1p in the wild-type cell. Therefore Abp1p localisation with both complexes appears to be independent of Sla1p. Interestingly, the small peak of cofilin that co-fractionates with the denser actin complexes completely disappears in the absence of Sla1p.

Localisation of Sla1p and Sla2p in wild-type and mutant strains

Sla1p and Sla2p localise to cortical patches, a subset of which contain actin (Ayscough et al., 1999; Yang et al., 1999). In order to examine the distribution of Sla1p-myc and Sla2p, a co-immunofluorescence experiment was carried out (Fig. 5A). Cells are shown that represent different stages within the cell cycle of budding yeast. Both Sla1p-myc- and Sla2p-containing patches were polarised to the site of bud emergence, to the enlarging bud and to the bud neck (Fig. 5A). Furthermore, Sla1p and Sla2p showed substantial colocalisation throughout the cell cycle. However, it was also apparent that a number of cortical patches contained only Sla1p-myc and rather fewer appeared to contain Sla2p alone, which suggests that colocalisation was not always complete.

Deletion of the entire *SLA1* coding region abrogated the interaction of Sla2p with the actin cytoskeleton (Ayscough et al., 1999), but our work detailed above shows that the interaction is mediated in vitro and in a two-hybrid assay by

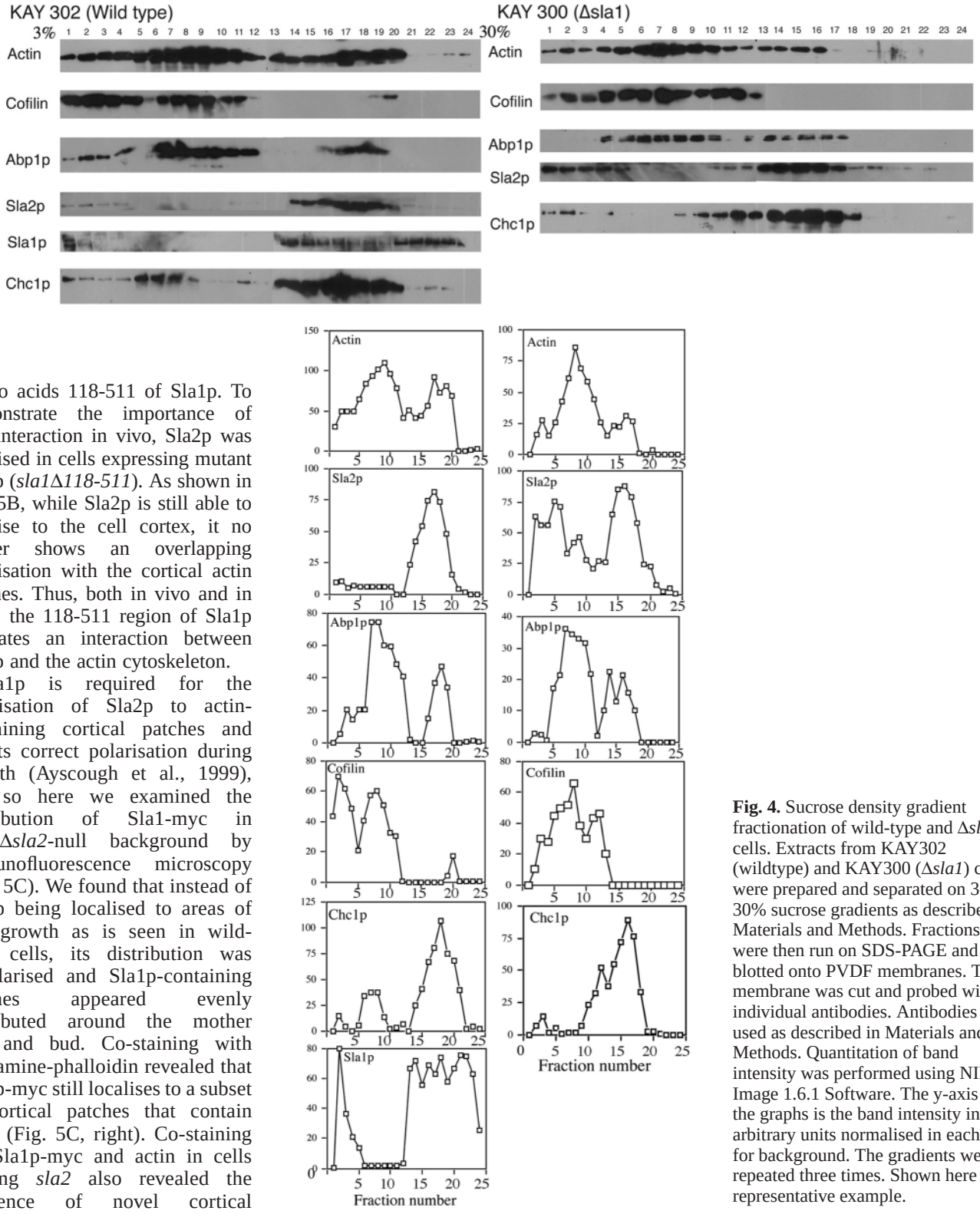

Fig. 4. Sucrose density gradient fractionation of wild-type and Δ*sla1* cells. Extracts from KAY302 (wildtype) and KAY300 (Δ*sla1*) cells were prepared and separated on 3-30% sucrose gradients as described in Materials and Methods. Fractions were then run on SDS-PAGE and blotted onto PVDF membranes. The membrane was cut and probed with individual antibodies. Antibodies were used as described in Materials and Methods. Quantitation of band intensity was performed using NIH Image 1.6.1 Software. The y-axis of the graphs is the band intensity in arbitrary units normalised in each case for background. The gradients were repeated three times. Shown here is a representative example.

amino acids 118-511 of Sla1p. To demonstrate the importance of this interaction in vivo, Sla2p was localised in cells expressing mutant Sla1p (*sla1Δ118-511*). As shown in Fig. 5B, while Sla2p is still able to localise to the cell cortex, it no longer shows an overlapping localisation with the cortical actin patches. Thus, both in vivo and in vitro, the 118-511 region of Sla1p mediates an interaction between Sla2p and the actin cytoskeleton.

Sla1p is required for the localisation of Sla2p to actin-containing cortical patches and for its correct polarisation during growth (Ayscough et al., 1999), and so here we examined the distribution of Sla1-myc in an Δ*sla2*-null background by immunofluorescence microscopy (Fig. 5C). We found that instead of Sla1p being localised to areas of cell growth as is seen in wild-type cells, its distribution was depolarised and Sla1p-containing patches appeared evenly distributed around the mother cell and bud. Co-staining with rhodamine-phalloidin revealed that Sla1p-myc still localises to a subset of cortical patches that contain actin (Fig. 5C, right). Co-staining for Sla1p-myc and actin in cells lacking *sla2* also revealed the existence of novel cortical structures. Normally actin and Sla1p, when colocalised, show an apparently tight overlap (Warren et al., 2002). In the structures shown in Fig. 5C Sla1p and actin only partially overlap and Sla1p appears to be mostly localised at the cortex of the cell, whereas actin appears to localise on the cytoplasmic side of the structures (Fig. 5C, inset).

Overexpression of Sla1(118-511) causes defects in endocytosis and membrane trafficking

The coiled-coil domain of Sla2p interacts with clathrin light chain (Henry et al., 2002). Because Sla1p also interacts with this region of Sla2p, we reasoned that overexpression of

Sla1(118-511ΔSH3#3) might interfere with other functions of Sla2p requiring this domain. Cells induced by growth in galactose to overexpress Sla1(118-511ΔSH3#3) were assessed for their ability to endocytose the dye lucifer yellow. As shown in Fig. 6A,B, a very marked phenotype is observed. There is a

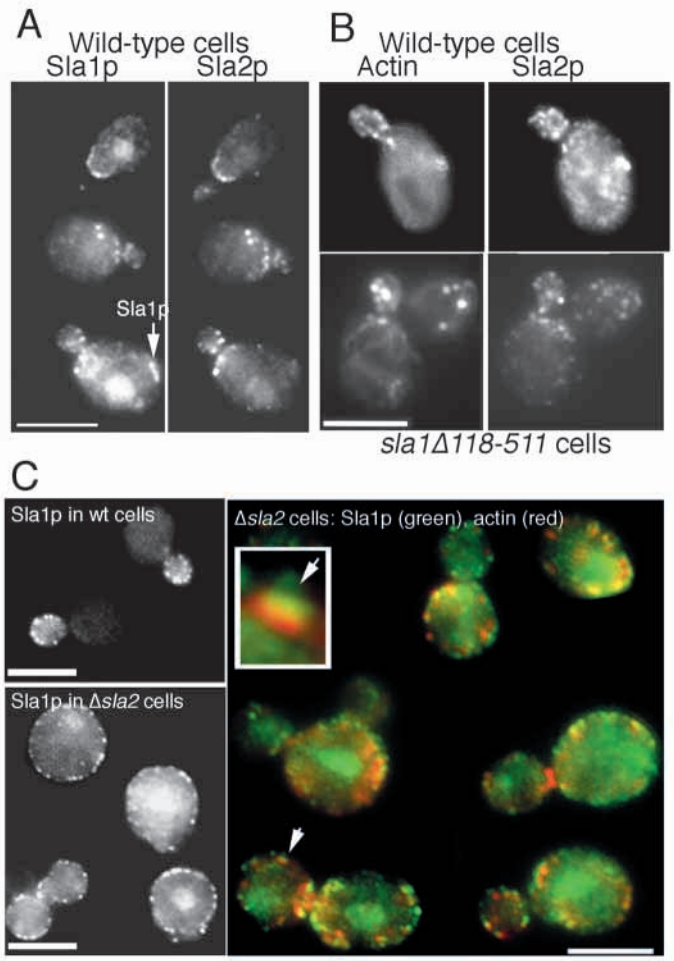

Fig. 5. Localisation of Sla1p and Sla2p in wild-type and mutant cells. (A) KAY303 cells expressing Sla2p and Sla1-myc were grown to log phase and processed for immunofluorescence microscopy as described in Materials and Methods. Both Sla1p-myc-containing and Sla2p-containing patches were polarised to the site of bud emergence, to the enlarging bud and to the bud neck. Furthermore, Sla1p and Sla2p showed substantial co-localisation throughout the cell cycle. However, as indicated by arrows, it was also apparent that a number of cortical patches contained only Sla1p-myc, which suggests that the colocalisation was not always complete. Bar, 10 μM. (B) KAY302 (wildtype) and KAY351 (Δ*sla1*Δ118-511) cells were grown to log phase and then fixed and processed for immunofluorescence microscopy as described in Materials and Methods. Actin was stained using rhodamine-phalloidin, and Sla2p was localised using antibodies raised to the protein. Bar, 10 μM. (C) The distribution of Sla1-myc in an Δ*sla2*-null background was examined using immunofluorescence microscopy. In wild-type cells Sla1p was localised to areas of active cell growth, whereas in the absence of *sla2* expression Sla1p distribution was depolarised and Sla1p-containing patches appeared evenly distributed around the mother cell and bud. Co-staining with rhodamine-phalloidin revealed that Sla1p-myc was still localised to a subset of cortical patches that contained actin. These images also suggested that in cells lacking Sla2p there are novel structures containing distinct regions of Sla1p and actin organisation (arrows). Bars, 10 μM. The inset shows part of the same image magnified two-fold, and the arrow points toward the same structure in both figures.

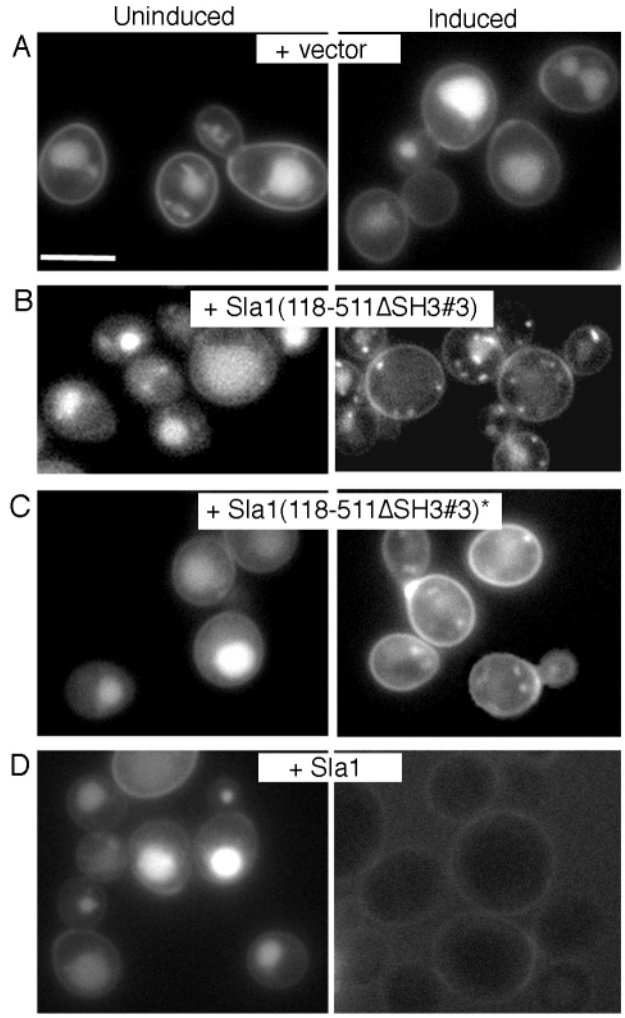

Fig. 6. Overexpression of Sla1(118-511) region disrupts fluid phase uptake of lucifer yellow and subsequent trafficking to the vacuole. Cells expressing GST alone (KAY439), GST-Sla1(118-511ΔSH3#3) (KAY508), GST-Sla1(118-511ΔSH3#3)* (KAY657) or GST-Sla1 (KAY439) were grown overnight in synthetic media containing 2% glucose, then inoculated into media with 2% galactose to induce expression of the various fusion proteins respectively. (A) Cells expressing GST alone displayed normal lucifer yellow uptake before and after induction and exhibited a strong fluorescence within the vacuole. (B) In cells induced to overexpress GST-Sla1p (118-511ΔSH3#3), lucifer yellow uptake was disrupted. These cells showed little vacuolar staining compared to those expressing GST alone and possessed more abundant brightly stained dots outside the vacuole. Lucifer yellow staining at the plasma membrane of these cells also appeared brighter than in the control cells. (C) A mutant form of Sla1 (118-511ΔSH3#3)* was expressed that cannot bind to another strong interactor of the 118-511 domain (Ysc84p). The same defect in uptake and subsequent trafficking was seen with this mutants with the Sla1(118-511ΔSH3#3) mutant, indicating that the defect is not because of the domain blocking normal Ysc84 function. (D) Overexpression of full-length Sla1p abrogated lucifer yellow uptake but did not result in accumulation of stained endosomes. Bar, 10 μM.

reduction in uptake of lucifer yellow to the vacuole coupled with an increase in staining of smaller organelles, potentially endosomes, as well as increased plasma membrane staining. Thus Sla1(118-511ΔSH3#3) overexpression causes reductions in both endocytosis and, interestingly, defects in subsequent trafficking to the vacuole. In order to determine whether this trafficking phenotype is largely due to Sla1(118-511) binding Sla2p but no longer being open to the regulation afforded by the presence of the rest of the molecule, two controls were performed. Firstly, full-length Sla1p was overexpressed. This caused a complete inhibition of endocytosis, and no endosomal staining was seen at all (Fig. 6D). Second, a mutant Sla1(118-511ΔSH3#3)* was expressed. This sequence contains a mutation rendering the domain unable to interact with Ysc84p, the other Sla1p-binding partner identified in the original two-hybrid screen (Dewar et al., 2002) (see also Materials and Methods and two-hybrid screen results). Cells expressing this mutant form of Sla1p sequence exhibited the same trafficking defect as in the Sla1(118-511ΔSH3) cells (Fig. 6C).

Over the time course of overexpression the actin phenotype was also monitored. Despite the endocytic defect, cells overexpressing either of the Sla1 fragments did not have an obviously disrupted actin phenotype, and the majority of actin was polarised in small punctate patches, which suggested that these cells are producing partially functional proteins. However, overexpression of the full-length sequence causes actin to aggregate into large cortical chunks, which produces an almost complete block in fluid phase endocytosis.

The Sla2p:Rvs167p interaction requires the presence of Sla1p

Work from other laboratories has demonstrated a two-hybrid interaction between Sla2p and one of the yeast amphiphysin homologues Rvs167p (Wesp et al., 1997). This interaction was postulated to facilitate the role of Sla2p in endocytosis. Rvs167p has also been reported to be an actin-associated protein (Cid et al., 1995). To address whether Rvs167p association with Sla2p occurred in the absence of Sla1p, we observed the localisation of Rvs167p in wild-type cells and in cells expressing the *sla1* deletion mutant (Fig. 7). In wild-type cells there was a partial overlap between Rvs167p and actin localisation, whereas in the Δ*sla1* cells Rvs167p colocalises completely with F-actin structures. From our previous data (Ayscough et al., 1999) and the data in Fig. 5B, we have shown that Sla2p does not colocalise with actin in the *sla1* deletion strain. Therefore, because Rvs167p colocalises with actin under these conditions, its association with Sla2p is likely to occur after the interaction between Sla1p and Sla2p.

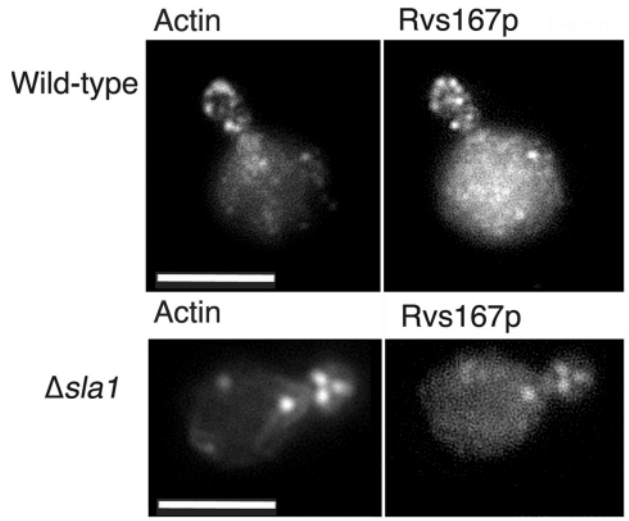

Fig. 7. Rvs167p localises with actin and not Sla2p in Δ*sla1* cells. KAY302 (wild-type) and KAY 97 (Δ*sla1*) cells were processed for immunofluorescence microscopy as described in Materials and Methods. Actin was stained using rhodamine-phalloidin, and Rvs167p was localised using antibodies raised against the protein. Although actin organisation is altered in the *sla1*Δ strain, Rvs167p still localises to these aberrant structures, which suggests that its association with actin is not mediated by Sla1p. Bar, 10 μM.

Characterisation of Δ*sla1*Δ*sla2* double mutant cells

To characterise the combined role played by Sla1p and Sla2p further, yeast strains were generated that did not expression both proteins, and the growth and morphology of these cells was analysed. Δ*sla1*Δ*sla2* double mutant cells appeared to grow at a similar rate and possessed a similar temperature-sensitive phenotype to that of Δ*sla2* cells. However, comparisons between Δ*sla1*Δ*sla2* double mutants with wild-type, Δ*sla1* or Δ*sla2* cells revealed a unique cold-sensitive phenotype only when both Sla1p and Sla2p are absent (results are summarised in Table 3). The significance of this double mutant phenotype is not known at present, although cold sensitivity has been associated with mutations in proteins involved in forming multi-subunit complexes (Moir et al., 1982). It was also noted that the Δ*sla1*Δ*sla2* cells were increased in cell volume compared with either Δ*sla1* or Δ*sla2* cells. The volume of cells grown at 29°C was measured using a Schärfe CASY™ cell counter and the mean volume of wild-type cells is 5.76 fl and Δ*sla1*Δ*sla2* cells is 13.8 fl. These data are summarised in Table 3.

We have shown previously that the deletion of *sla1* and *sla2* individually influences the sensitivity of yeast to the actin-disrupting drug Latrunculin-A (LAT-A). Because LAT-A binds to actin monomers, sensitivity to the drug can be related to whether a protein increases or decreases the stability of F-actin in cells. When LAT-A was administered to cells in culture, as described previously, deletion of *sla1* reduces the sensitivity to LAT-A whereas Δ*sla2* cells are more sensitive to the effects of the drug (Ayscough et al., 1999; Warren et al., 2002). However, the double mutant cells displayed an intermediate phenotype, being more sensitive than Δ*sla1* cells but less so than the Δ*sla2* mutant (data not shown). A similar result was obtained when LAT-A sensitivity was assessed by a halo assay approach. A summary of the halo assay data is shown in Fig. 8A.

Table 3. Phenotypes of Δ*sla1*Δ*sla2* cells

Strains	Temperature sensitivity 16°C	30°C	37°C	Growth on YP + 3% glycerol	Cell size (fl)
Wildtype	+++	+++	+++	+++	5.86
Δ*sla1*	++	++	+/–	+/–	6.83
Δ*sla2*	++	++	–	++	9.24
Δ*sla1*Δ*sla2*	+/–	++	–	–	13.8

Actin patch organisation in Δ*sla1*Δ*sla2* cells

The most striking phenotype of Δ*sla1*Δ*sla2* double mutant cells is observed when the actin cytoskeleton is stained with rhodamine-phalloidin. Fig. 8B shows F-actin staining in wildtype, cells with deletions of either Δ*sla1* or Δ*sla2* or both Δ*sla1* and Δ*sla2*. Wild-type cells demonstrated polarisation of the actin cytoskeleton to sites of cell growth. In Δ*sla1* cells, cortical actin patches appeared larger than those in wildtype, were fewer and were less well polarised. In Δ*sla2* mutant cells the documented phenotype of smaller, more numerous, actin patches that were distributed evenly throughout the mother cell and bud was seen (Holtzman et al., 1993). In Δ*sla1*Δ*sla2* double mutant cells a novel phenotype was observed. Cortical actin patches were primarily polarised to the distal end of the mother cell. In these cells, small, less brightly stained patches could often be seen at polarised regions of the cell (arrows) and an actin ring could be seen at the site of cytokinesis (arrowheads), but this represented a small fraction of actin that was visualised (Fig. 8B lower panel). The organisation of actin in the Δ*sla1*Δ*sla2* cells was unexpected as it appears to be opposite from the cell polarity as defined by the sites of bud growth. However, in these cells, budding appears to occur relatively normally and tubulin staining of cytoplasmic microtubules and the mitotic spindle is not aberrant (data not shown).

To determine whether the distally localised F-actin patches contained a normal complement of actin-binding proteins we used immunofluorescence microscopy to determine the localisation of the yeast fimbrin homologue Sac6p and the actin-binding protein Abp1p (Fig. 8C,D). Both of these proteins normally localise to cortical actin patches, and their localisation to the distally located actin patches in the Δ*sla1*Δ*sla2* cells indicates that this actin is likely to be folded correctly.

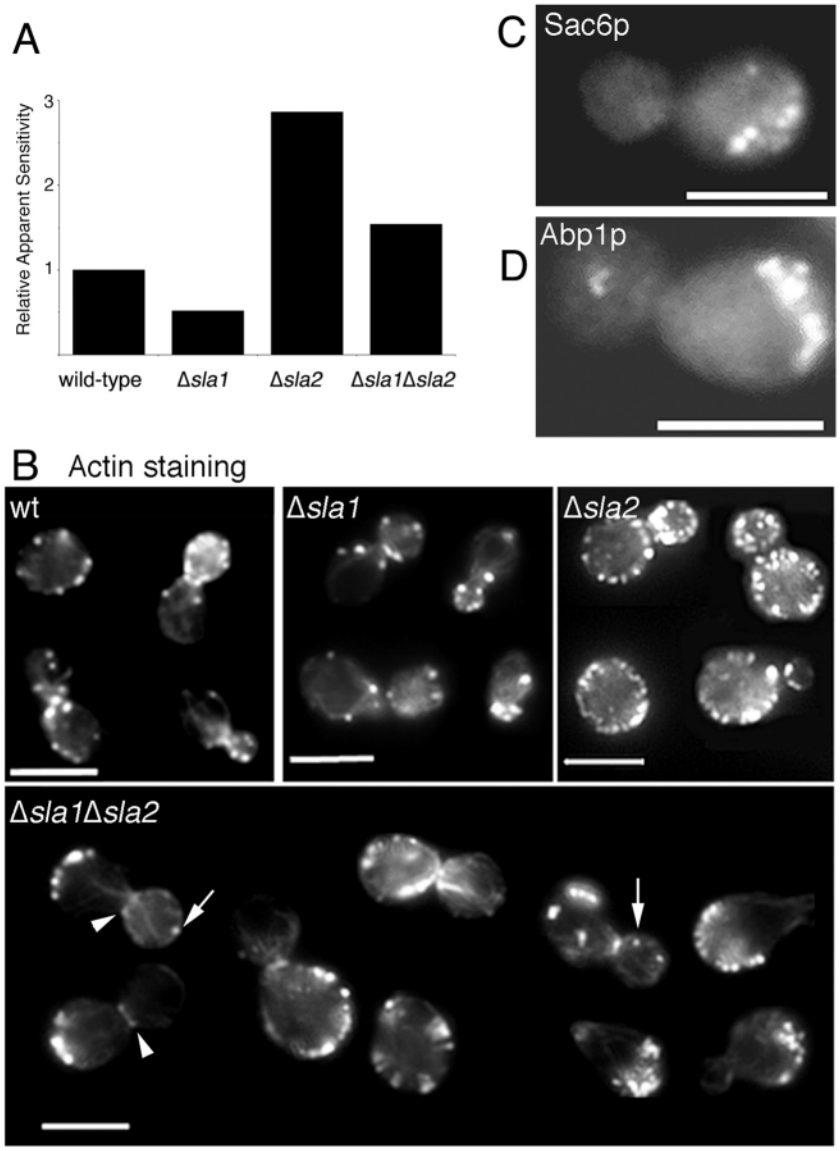

Fig. 8. The actin phenotypes of Δ*sla1*Δ*sla2* cells. (A) Sensitivity to the actin monomer binding drug LAT-A is proposed to reflect the level of actin monomer in cells and therefore can be used to assess to whether a protein increases or decreases the stability of F-actin. Sensitivity to LAT-A was assessed by halo assay as described in Materials and Methods. These results are summarised graphically. Deletion of *sla1* reduces the sensitivity to LAT-A whereas Δ*sla2* cells are more sensitive to the effects of the drug. The double mutant strains displayed an intermediate phenotype. The data shown are the average of three halo assays. Strains tested were KAY302, KAY97, KAY136 and KAY128. (B) Rhodamine-phalloidin was used to stain the F-actin of wild-type (KAY302), Δ*sla1* (KAY97), Δ*sla2* (KAY136) and Δ*sla1*Δ*sla2* (KAY128) cells. In the absence of both sla1p and Sla2p, actin is largely localised to the distal pole of the cell. However, in these cells small, less bright patches could often be seen at polarised regions of the cell (arrows), and actin was also seen at the cytokinetic ring (arrowheads) but this represented a small fraction of the actin that was visualised. Bar, 10 μm. To ascertain whether this larger aggregation of actin patches was likely to be functional, the localisation of two F-actin-binding proteins was determined. Both Sac6p (C) and Abp1p (D) were also observed to localise to the distal regions of the cell, indicating that the actin in these structures is associated with a normal complement of actin-binding proteins. Bar, 10 μm.

Endocytosis and membrane trafficking in Δ*sla1*Δ*sla2* cells

Defects in endocytosis have been reported in both Δ*sla1* and Δ*sla2* single mutant strains. The effect of *sla1* deletion on fluid phase uptake of the fluorescent dye lucifer yellow is not absolute, with about 30% of cells showing no uptake and 60-70% of cells showing a reduction in uptake of the dye (Warren et al., 2002). Sla2p appears to play a more critical role in endocytosis with most cells showing only a low level of lucifer yellow uptake (Fig. 9A) (Raths et al., 1993). The Δ*sla1*Δ*sla2* cells show a phenotype that is more severe than the Δ*sla2* strain, and we observed less than 1% of cells with any fluid phase uptake of the dye. The percentage of cells showing vacuolar staining was

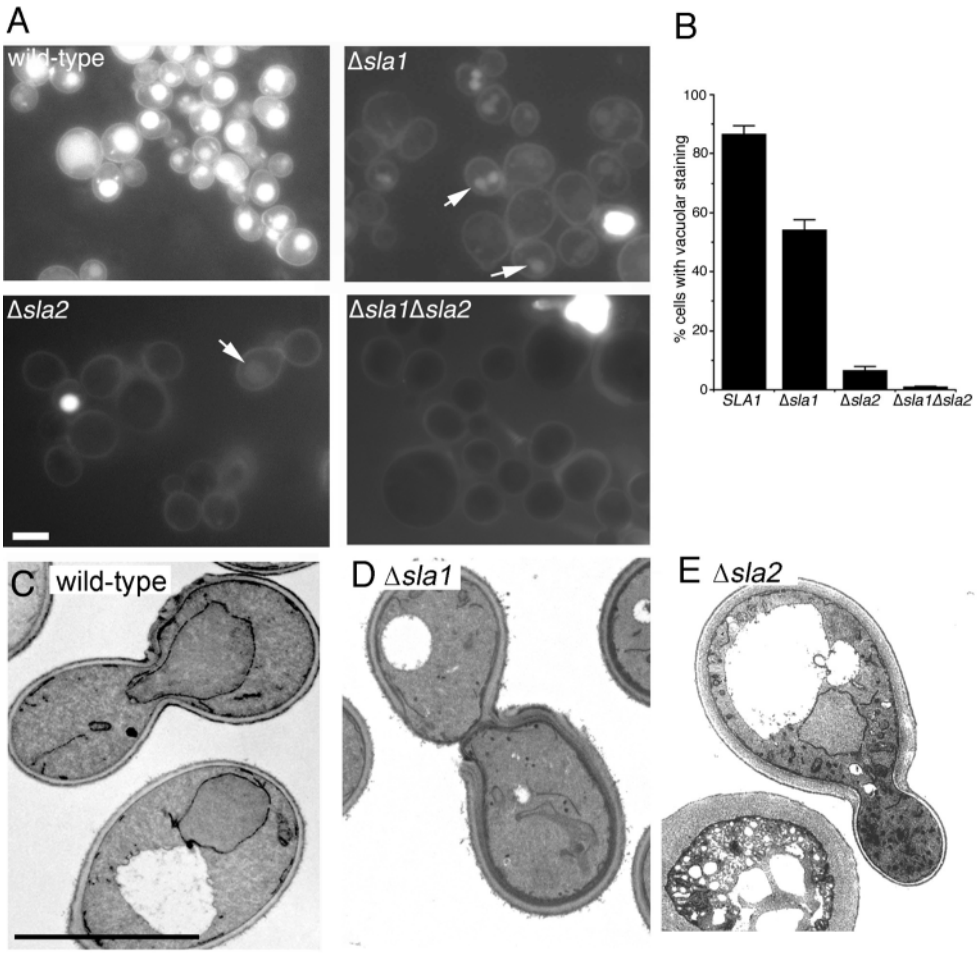

Fig. 9. Endocytosis and membrane trafficking in Δ*sla1*Δ*sla2* cells. (A) Fluid phase endocytosis was monitored by following uptake of the fluorescent dye lucifer yellow (see Materials and Methods). Wild-type cells show uptake of the dye into vacuoles. Over the same time period Δ*sla1* cells show a reduction in uptake whereas Δ*sla2* and the Δ*sla1*Δ*sla2* cells show little or no detectable internalisation of the dye. Bar, 10 μm. The percentage of cells showing detectable uptake of the dye into vacuoles is summarised graphically in B. 200 cells were counted in each of three experiments. Error bars represent standard error. (C) Wild-type (D) Δ*sla1*, (E) Δ*sla2* and (F) Δ*sla1*Δ*sla2* cells were processed for electron microscopy using potassium permanganate as described in Materials and Methods. Bar, 5 μm.

assessed for all strains; this is summarised graphically in Fig. 9B and all experiments were performed three times, counting 200 cells of each strain on every occasion.

Uptake of the dye FM4-64 was also monitored in wild-type and mutant cells. This dye can be used to study mutants that have defects in membrane trafficking in addition to in the initial internalisation step of endocytosis (Vida and Emr, 1995). All of the mutant strains showed a kinetic delay in FM4-64 uptake, although by 60 minutes, labelling was similar to that found in wild-type cells. Wild-type cells showed vacuolar staining after 15 minutes, Δ*sla1* and Δ*sla2* after 25 minutes and Δ*sla1*Δ*sla2* cells showed vacuolar staining after 35 minutes, although this was weaker than in the wild-type or single mutant strains.

Finally we used electron microscopy to investigate whether there were any marked changes in number or organisation of membrane structures. Previously, Δ*sla2* cells were shown to accumulate vesicles in the bud (Mulholland et al., 1997). As shown in Fig. 9C-F, there is a clear increase in the number of vesicles in both Δ*sla2* and Δ*sla1*Δ*sla2* cells. One difference however between these two mutants is that the vesicles in the double mutant appear to accumulate in both the mother and bud, whereas the vesicles in the Δ*sla2* mutant appear mostly to localise to the bud.

Discussion

The work presented here provides new insights into the interactions between the endocytic machinery and the proteins of the cortical actin cytoskeleton. We show that Sla1p binds to Sla2p both in vivo and in vitro. We also demonstrate that this interaction is mediated by amino acids 118-361 of Sla1p and the region 310-768 of Sla2p, which encompasses its central

coiled-coil domain. The interaction does not require the third SH3 domain of Sla1p. The central domain of Sla2p, which includes two regions with coiled-coil structure, has previously been shown to be important for its role in endocytosis (Wesp et al., 1997) and has been reported to interact with the actin-regulating kinase Ark1p (Cope et al., 1999). More recently this domain has been shown to interact with clathrin light chain (Henry et al., 2002).

On the basis of the data shown above, previous work in our laboratory and work from other laboratories, we believe that current data are consistent with the following model for the role of the interaction of Sla1p and Sla2p in coupling cortical actin to endocytosis. It should be noted, however, that this model does not aim to be all inclusive and that both proteins are also likely to make interactions with other proteins at the cell cortex that may also play a role in the endocytic process. Our model is summarised in Fig. 10. Numbers indicate potentially sequential interactions.

(1) Sla2p associates with clathrin light chain at sites marked for endocytosis. This localisation to the cortex may also be mediated by the Sla2p ENTH domain, which is likely to interact with PtdIns(4,5)P_2 in the membrane. The demonstration that deletion of *SLA2* results in loss of both actin and Sla1p polarity (Fig. 5) strongly implicates Sla2p localisation at the cortex as an early step in the process of endocytosis (Holtzman, 1993; Henry et al., 2002).

(2) Sla2p is then able to bind to Sla1p, which itself is already complexed to Pan1p and End3p (Zeng et al., 2001). Sla1p does not appear to be recruited from the cytosol to the Sla2p sites; rather it is found in pre-existing complexes at the plasma membrane that are distinct from both Sla2p (Fig. 5A) and actin complexes (Warren et al., 2002).

(3) Sla2p in association with Sla1p, End3p and Pan1p may then recruit actin patches. Sla1p binds to the Arp2/3-activating protein Abp1p (Warren et al., 2002) and Las17/Bee1p (Li, 1997; Warren et al., 2002). Pan1p has been shown to associate with Arp2/3 (Duncan et al., 2001). These interactions (and most probably others) then facilitate cycles of actin assembly and disassembly, which allow reorganisation of the actin cytoskeleton, which in turn promote endocytosis.

In Δ*sla2* cells, Sla1p cannot localise to the endocytic sites, which in turn means there is no actin recruitment to these sites. This results in a very significant reduction in levels of endocytosis. The loss of Δ*sla1* is rather more subtle, possibly because there are proteins with roles that partially overlap with that of Sla1p. In the absence of Sla1p there is an increase in F-actin, visualised as fewer larger chunks of actin in cells (Holtzman et al., 1993). This correlates to a reduction but not total abrogation of endocytosis (Warren et al., 2002). The effect of *sla1* deletion on F-actin organisation indicates that the Sla1p interaction with the Arp2/3 activators Abp1p and Las17/Bee1p may be inhibitory. In wild-type cells, Sla1p may downregulate actin polymerisation and thereby result in net depolymerisation. Thus, when Sla1p is absent, there is an imbalance in actin assembly and disassembly rates, and this leads to accumulation of actin chunks, which are relatively stable However, there is possibly still some level of actin dynamics that means that endocytosis is not completely prevented. It is interesting to speculate from the sucrose density gradient analysis (Fig. 4) that the absence of cofilin from large protein complexes may serve to partly explain the lack of depolymerisation in the absence of Sla1p.

The observation that Sla1p and Sla2p proteins have opposite effects on actin dynamics in cells even though they are found in overlapping complexes is likely to be crucial (Fig. 5). As mentioned above, deletion of *sla1* causes cells to become resistant to the effects of LAT-A, which indicates that it normally has a destabilising effect on F-actin, whereas deletion of *sla2* causes a marked increase in sensitivity to LAT-A, suggesting a role for Sla2p in stabilising F-actin (Ayscough et al., 1997) (Fig. 8A). Actin rearrangements require both disassembly of existing structures (therefore a destabilising/disassembling activity is required) and subsequently reassembly into new structures (requiring nucleating/stabilising properties). Talin has been shown to stabilise F-actin structures (Hemmings et al., 1996; Priddle et al., 1998) and so it is possible that the talin homology region of Sla2p may perform a similar role to this mammalian protein. The Sla2p actin-binding function appears to be masked by intramolecular interactions that have been demonstrated to be due to sequences within the central domain (Yang et al., 1999). This Sla2p domain, however, appears to be involved in a number of interactions. As well as interacting with itself to form a dimer, associations have also been reported with clathrin light chain (Henry et al., 2002), the actin-regulating kinase Ark1p (Cope et al., 1999) and, as described here, with Sla1p. It is possible that association with one or more of these proteins leads to unmasking of the actin-binding site, which then facilitates formation of actin structures that favour endocytosis.

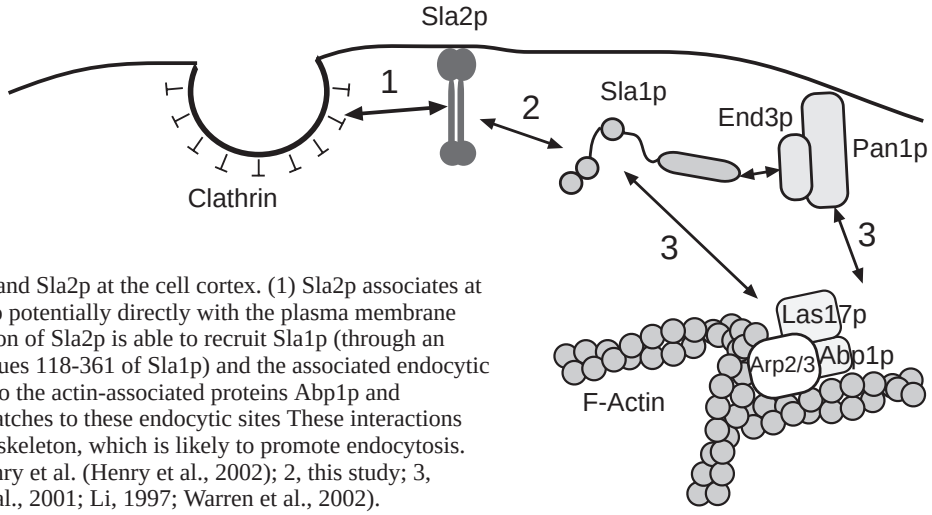

Fig. 10. Model depicting interactions of Sla1p and Sla2p at the cell cortex. (1) Sla2p associates at the cell cortex with clathrin light chain and also potentially directly with the plasma membrane through its ENTH domain. (2) The central region of Sla2p is able to recruit Sla1p (through an interaction with a region encompassed by residues 118-361 of Sla1p) and the associated endocytic machinery Pan1p/End3p. (3) Sla1p also binds to the actin-associated proteins Abp1p and Las17p/Bee1p, allowing recruitment of actin patches to these endocytic sites These interactions then lead to the reorganisation of the actin cytoskeleton, which is likely to promote endocytosis. Evidence for these is from these studies: 1, Henry et al. (Henry et al., 2002); 2, this study; 3, Duncan et al., Li and Warren et al. (Duncan et al., 2001; Li, 1997; Warren et al., 2002).

We also show that overexpression of the Sla1-Sla2 interaction domain (Sla1-118-511) can block both endocytosis and membrane trafficking to the vacuole. This suggests that Sla1p and Sla2p must normally become dissociated for endocytosis to proceed. Work by Zeng and colleagues has indicated that phosphorylation of the C-terminal region of Sla1p by the actin-regulating kinase Prk1p causes it to dissociate from cortical complexes (Zeng et al., 2001). This may then be a pre-requisite for endocytosis. In our experiment the fragment Sla1(118-511) cannot be regulated by Prk1p because it lacks the C-terminal motifs that become phosphorylated. It may therefore continue to associate with the endocytic complex, presumably blocking interactions that are required for endocytosis to proceed. Interestingly, there appears to be a low level of fluid phase uptake of the dye, into small organelles, which may be endosomes. Alternatively, these structures could be similar to the previously reported finger-like invaginations, which may not have yet pinched off from the plasma membrane (Wendland et al., 1996). This result may suggest that proteins with which Sla1p/Sla2p interact also act downstream of the initial endocytosis events.

Finally, we report the consequences of combining the Δ*sla1* and Δ*sla2* mutations in cells. This leads to a complete block in fluid phase endocytosis and also to a novel actin phenotype in which the majority of F-actin is localised to the distal pole of the cell. The reason for this organisation of cortical actin is not clear. It does however illustrate that lack of polarised cortical actin does not abrogate polarised growth of cells and adds further support to the importance of actin cables rather than cortical actin patches in generating and maintaining cell polarity through directed cell growth (Evangelista et al., 2002; Sagot et al., 2002)

The role of actin in the process of endocytosis is not yet clear. However, studies in mammalian cells have shown that depolymerisation of F-actin can increase the lateral movement of clathrin-coated pits, which suggests that the actin cytoskeleton provides a scaffold at the plasma membrane for the endocytic machinery (Gaidarov et al., 1999). Other ideas for the role of actin include a role in invagination of the membrane, fission of the vesicle or movement of the vesicle into the cell (reviewed in Qualmann et al., 2000). The data we present here suggest that actin is not required for the initial marking of the site of endocytosis. Rather it is required to be dynamic and is rearranged at sites of endocytosis. Potentially it is these rearrangements that drive formation of the vesicle or its inward movement into the cell.

We are grateful to Steve Winder and Fiona Gardiner for critical reading of the manuscript, to Margaret Mullin for assistance with electron microscopy, to Jamie Cope and David Drubin (UC Berkeley) for the GST-Sla1p and Sla2-His plasmids, to David Drubin for the pACTII *Sla2* two hybrid plasmids and for Abp1p, Sac6p and Sla2p antibodies, to Helen Friesen (University of Toronto) for the Rvs167p antibody, to Sandra Lemmon (Cleveland, Ohio) for the Chc1 antibody, to Francis Barr for the two-hybrid library and to Phil Crews (UC Santa Cruz) for Latrunculin-A. This work was supported by an MRC Senior non-clinical Fellowship to K.R.A. (G117/394) and an award from The Wellcome Trust (050934/Z/97).

References

Adams, **A. E. M. and Pringle, J. R.** (1984). Relationship to actin and tubulin distribution to bud growth in wild type and morphogenetic mutant *Saccharomyces cerevisiae*. *J. Cell Biol*. **98**, 934-945.

Ayscough, K. R. (1998). *In vivo* functions of actin-binding proteins. *Curr. Opin. Cell Biol*. **10**, 102-111.

Ayscough, K. R. and Drubin, D. G. (1998). Immunofluorescence Microscopy of Yeast Cells. In *Cell Biology: A Laboratory Handbook.* Vol. 2 (ed. J. Celis), pp. 477-485. New York: Academic Press.

Ayscough, K. R., Stryker, J. Pokala, N. Sanders, M. Crews, P. and Drubin, D. G. (1997). High rates of actin filament turnover in budding yeast and roles for actin in establishment and maintenance of cell polarity revealed using the actin inhibitor latrunculin-A. *J. Cell Biol*. **137**, 399-416.

Ayscough, K. R., Eby, J. J., Lila, T., Dewar, H., Kozminski, K. G. and Drubin, D. G. (1999). Sla1p is a functionally modular component of the yeast cortical actin cytoskeleton required for correct localization of both Rho1p-GTPase and Sla2p, a protein with talin homology. *Mol. Biol. Cell* **10**, 1061-1075.

Cid, V. J., Duran, A., del Rey, F., Snyder, M. P., Nombela, C. and Sanchez, M. (1995). Molecular basis of cell integrity and morphogenesis in *Saccharomyces cerevisiae*. *Microbiol. Rev*. **59**, 345-386.

Cope, M. J. V., Yang, S., Shang, C. and Drubin. D. G. (1999). Novel protein kinases Ark1p and Prk1p associate with and regulate the cortical actin cytoskeleton in budding yeast. *J. Cell Biol*. **144**, 1203-1218.

De Camilli, P., Chen, H., Hyman, J., Panepucci, E., Bateman, A. and Brunger, A. T. (2002). The ENTH domain. *FEBS Lett*. **513**, 11-18.

Dewar, H., Warren, D. T., Gardiner, F. C., Gourlay, C. G., Satish, N., Richardson, M. R., Andrews, P. D. and Ayscough. K. R. (2002). Novel proteins linking the actin cytoskeleton to the endocytic machinery in *Saccharomyces cerevisiae*. *Mol. Biol. Cell* **13**, 3646-3661.

Drubin, D. G., Miller, K. G. and Botstein, D. (1988). Yeast actin binding proteins: Evidence for a role in morphogenesis. *J. Cell Biol*. **107**, 2551-2561.

Dulic, V., Egerton, M., Elgundi, I., Raths, S., Singer, B. and Riezman, H. (1991). Yeast endocytosis assays. *Meth. Enzymol*. **194**, 697-710.

Duncan, M. C., Cope, M., Goode, B. L., Wendland, B. and Drubin, D. G. (2001). Yeast Eps15-like endocytic protein, Pan1p, activates the Arp2/3 complex. *Nat. Cell Biol*. **3**, 687-690.

Engqvist-Goldstein, A. E. Y., Kessels, M. M., Chopra, V. S., Hayden, M. R. and Drubin, D. G. (1999). An actin-binding protein of the Sla2/Huntingtin interacting protein 1 family is a novel component of clathrin-coated pits and vesicles. *J. Cell Biol*. **147**, 1503-1518.

Engqvist-Goldstein, A. E. Y., Warren, R. A., Kessels, M. M., Keen, J. H., Heuser, J. and Drubin, D. G. (2001). The actin-binding protein Hip1R associates with clathrin during early stages of endocytosis and promotes clathrin assembly in vitro. *J. Cell Biol*. **154**, 1209-1223.

Evangelista, M., Pruyne, D., Amberg, D. C., Boone, C. and Bretscher, A. (2002). Formins direct Arp2/3 independent actin filament assembly to polarize cell growth in yeast. *Nat. Cell Biol*. **4**, 32-41.

Gaidarov, I., Santini, F., Warren, R. A. and Keen, J. H. (1999). Spatial control of coated-pit dynamics in living cells. *Nat. Cell Biol.* **1**, 1-7.

Hagan, I. M. and Ayscough, K. R. (2000). Fluorescence Microscopy in Yeast. *In Protein Localization by Fluorescence Microscopy: A Practical Approach* (ed. V. J. Allan), pp. 179-205. Oxford: Oxford University Press.

Hemmings, L., Rees, D. J. G., Ohanian, V., Bolton, S. J., Gilmore, A. P., Patel, B., Priddle, H., Trevithick, J. E., Hynes, R. O. and Critchley, D. R. (1996). Talin contains three actin-binding sites each of which is adjacent to a vinculin-binding site. *J. Cell Sci*. **109**, 2715-2726.

Henry, K., D'Hondt, K., Chang, J., Newpher, T., Huang, K., Hudson, R., Riezman, H. and Lemmon, S. (2002). Scd5p and clathrin function are important for cortical actin organisation, endocytosis and localisation of Sla2p in yeast. *Mol. Biol. Cell* **13**, 2607-2625.

Holtzman, D. A., Yang, S. and Drubin, D. G. (1993). Synthetic-lethal interactions identify two novel genes, *SLA1* and *SLA2*, that control membrane cytoskeleton assembly in *Saccharomyces cerevisiae*. *J. Cell Biol*. **122**, 635-644.

James, P., Halladay, J. and Craig, E. A. (1996). Genomic libraries and a host strain designed for highly efficient two-hybrid selection in yeast. *Genetics* **144**, 1425-1436.

Kessels, M. M., Engqvist-Goldstein, A. E. Y., Drubin, D. G. and Qualmann, B. (2001). Mammalian Abp1, a signal-responsive F-actin-binding protein, links the actin cytoskeleton to endocytosis via the GTPase dynamin. *J. Cell Biol*. **153**, 351-366.

Kübler, E. and Riezman, H. (1993). Actin and fimbrin are required for the internalization step of endocytosis in yeast. *EMBO J*. **12**, 2855-2862.

Li, R. (1997). Bee1, a yeast protein with homolgy to Wiscott-Aldrich

syndrome protein, is critical for the assembly of cortical actin cytoskeleton. *J. Cell Biol.* **136**, 649-658.

McCann, R. O. and Craig. S. W. (1997). The I/LWEQ module: A conserved sequence that signifies F-actin binding in functionally diverse proteins from yeast to mammals. *Proc. Natl. Acad. Sci. USA* **94**, 5679-5684.

Moir, D., Stewart, S. E., Osmond, B. C. and Botstein. D. (1982). Cold-sensitive cell-division-cycle mutants of yeast – isolation, properties, and pseudo-reversion studies. *Genetics* **100**, 547-563.

Mulholland, J., Wesp, A., Riezman, H. and Botstein, D. (1997). Yeast actin cytoskeleton mutants accumulate a new class of Golgi-derived secretory vesicle. *Mol. Biol. Cell* **8**, 1481-1499.

Novick, P. and Botstein. D. (1985). Phenotypic analysis of temperature sensitive yeast actin mutants. *Cell* **40**, 405-416.

Priddle, H., Hemmings, L., Monkley, S., Woods, A., Patel, B., Sutton, D., Dunn, G., Zicha, D. and Critchley, D. (1998). Disruption of the talin gene compromises focal adhesion assembly in undifferentiated but not differentiated embryonic stem cells. *J. Cell Biol*. **142**, 1121-1133.

Qualmann, B., Kessels, M. M. and Kelly, R. B. (2000). Molecular links between endocytosis and the actin cytoskeleton. *J. Cell Biol*. **150**, F111-F116.

Raths, S., Rohrer, J., Crausaz, F. and Riezman, H. (1993). end3 and end4: two mutants defective in receptor-mediated endocytosis in *Saccharomyces cerevisiae*. *J. Cell Biol*. **120**, 55-65.

Sagot, I., Klee, S. K. and Pellman, D. (2002). Yeast formins regulate cell polarity by controlling the assembly of actin cables. *Nat. Cell Biol*. **4**, 42-50.

Simon, V. R., Karmon, S. L. and Pon, L. A. (1997). Mitochondrial inheritance: Cell cycle and actin cable dependence of polarized mitochondrial movements in *Saccharomyces cerevisiae*. *Cell Motil. Cytoskeleton* **37**, 199-210.

Vida, T. and Emr, S. (1995). A new vital stain for visualizing vacuolar membrane dynamics and endocytosis in yeast. *J. Cell Biol*. **128**, 779-792.

Warren, D. T., Andrews, P. D., Gourlay, C. G. and Ayscough, K. R. (2002). Sla1p couples the yeast endocytic machinery to proteins regulating actin dynamics. *J. Cell. Sci.* **115**, 1703-1715.

Wendland, B., McCaffery, J. M., Xiao, Q. and Emr, S. D. (1996). A novel fluorescence-activated cell sorter-based screen for yeast endocytosis mutants identifies a yeast homologue of mammalian eps15. *J. Cell Biol* **135**, 1485-1500.

Wesp, A., Hicke, L., Palecek, J., Lombardi, R., Aust, T., Munn, A. L. and Riezman, H. (1997). End4p/Sla2p interacts with actin-associated proteins for endocytosis in *Saccharomyces cerevisiae*. *Mol. Biol. Cell* **8**, 2291-2306.

Yang, S., Cope, M. and Drubin, D. G. (1999). Sla2p is associated with the yeast cortical actin cytoskeleton via redundant localization signals. *Mol. Biol. Cell* **10**, 2265-2283.

Zeng, G. H., Yu, X. W. and Cai, M. J. (2001). Regulation of yeast actin cytoskeleton-regulatory complex Pan1p/Sla1p/End3p by serine/threonine kinase Prk1p. *Mol. Biol. Cell* **12**, 3759-3772.